ISSN 1674-1056
http://cpb.iphy.ac.cn
http://iopscience.iop.org/cpb
中国物理 B
Chinese Physics
中国物理 Chinese Physics B

Multiple broadband magnetoelectric response in Terfenol-D/PZT structure

Jian-Biao Wen(文建彪)[1,2], Juan-Juan Zhang(张娟娟)[1,2], Yuan-Wen Gao(高原文)[1,2]
Citation: Chin. Phys. B . 2018, 27(2): 027702. **doi:** 10.1088/1674-1056/27/2/027702

Journal homepage: http://cpb.iphy.ac.cn; http://iopscience.iop.org/cpb

What follows is a list of articles you may be interested in

Multiferroic and enhanced microwave absorption induced by complex oxide interfaces

Cuimei Cao(曹翠梅), Chunhui Dong(董春晖), Jinli Yao(幺金丽), Changjun Jiang(蒋长军)
Chin. Phys. B . 2018, 27(1): 017503. **doi:** 10.1088/1674-1056/27/1/017503

Modified magnetomechancial model in the constant and low intensity magnetic field based on J–A theory

Qingyou Liu(刘清友), Xu Luo(罗旭), Haiyan Zhu(朱海燕), Jianxun Liu(刘建勋), Yiwei Han(韩一维)
Chin. Phys. B . 2017, 26(7): 077502. **doi:** 10.1088/1674-1056/26/7/077502

Giant low-frequency magnetoelectric torque (MET) effect in polyvinylidene-fluoride (PVDF)-based MET device

Chun-Lei Zheng(郑春蕾), Yi-Wei Liu(刘宜伟), Qing-Feng Zhan(詹清峰), Yuan-Zhao Wu(巫远招), Run-Wei Li(李润伟)
Chin. Phys. B . 2017, 26(6): 067703. **doi:** 10.1088/1674-1056/26/6/067703

Modeling of the loading path dependent magnetomechanical behavior of Galfenol alloy

Hui Jiang(江慧), Jie Zhu(朱洁)
Chin. Phys. B . 2017, 26(3): 037503. **doi:** 10.1088/1674-1056/26/3/037503

Review on graphene-based strain sensors

Zhao Jing, Zhang Guang-Yu, Shi Dong-Xia
Chin. Phys. B . 2013, 22(5): 057701. **doi:** 10.1088/1674-1056/22/5/057701

Multiple broadband magnetoelectric response in Terfenol-D/PZT structure*

Jian-Biao Wen(文建彪)[1,2], Juan-Juan Zhang(张娟娟)[1,2,†], and Yuan-Wen Gao(高原文)[1,2]

[1] *Key Laboratory of Mechanics on Disaster and Environment in Western China, The Ministry of Education of China, Lanzhou University, Lanzhou* 730000, *China*

[2] *Department of Mechanics and Engineering Science, College of Civil Engineering and Mechanics, Lanzhou University, Lanzhou* 730000, *China*

(Received 7 October 2017; revised manuscript received 17 November 2017; published online 29 January 2018)

In this paper, a novel magnetoelectric (ME) composite structure is proposed, and the ME response in the structure is measured at the bias magnetic field up to 2000 Oe (1 Oe = 79.5775 A·m^{-1}) and the excitation frequency of alternating magnetic field ranging from 1 kHz to 200 kHz. The ME voltage of each PZT layer is detected. According to the measurement results, the phase differences are observed among three channels and the multi-peak phenomenon appears in each channel. Meanwhile, the results show that the ME structure can stay a relatively high ME response within a wide bandwidth. Besides, the hysteretic loops of three PZT layers are observed. When the frequency of alternating current (AC) magnetic field changes, the maximum value of ME coefficient appears in different layers due to the multiple vibration modes of the structure. Moreover, a finite element analysis is performed to evaluate the resonant frequency of the structure, and the theoretical calculating results accord well with the experimental results. The experiment results suggest that the proposed structure may be a good candidate for designing broadband magnetic field sensors.

Keywords: ME effect, novel structure, multipeaks, broadband response

PACS: 77.65.Ly, 75.80.+q, 85.80.Jm, 75.85.+t **DOI:** 10.1088/1674-1056/27/2/027702

1. Introduction

The strong magnetoelectric (ME) coupling in multiferroic material has attracted lots of researchers to study because of its enormous potential in multifunctional devices.[1–3] For enhancing the ME coefficient in experiment, many inspiring ideas have been proposed, such as adopting different fabrication methods,[4–8] selecting different components,[9–12] and designing various configurations.[13–16] A relatively high ME coefficient can be expected from those methods. However, there are only a few peaks that can be observed in a wide frequency range, and the ME coupling stays poor performance at other frequencies, which restricts the application for stable sensing.

In order to overcome the shortcoming, many efforts have been made to obtain a wide ME response in ME composites by adopting different electric connections,[17,18] fabricating particular structures,[19–21] implementing different mechanical boundary conditions,[22] and using anisotropic piezoelectric materials.[23] A broadband ME response can be achieved in those researches, but the ME coefficient is reduced or the resonant frequency is too high, which is not suitable for detecting low frequency alternating current (AC) magnetic field. Thus, it is urgent to find a feasible approach to maintaining good performance in a wide range of low frequency.

For the same purpose, we design a novel structure in this study, which is made up of one magnetostrictive layer and three piezoelectric layers. They connect with a trestle that is nonmagnetic and nonelectric. Compared with the traditional ME structure, the three piezoelectric layers in the novel ME structure can be driven by only one magnetostrictive layer. Through experimental measurements, a broad ME response can be obtained in a low frequency range, meanwhile a finite element modeling analysis is conducted to estimate the resonant frequencies. The results indicate the ME structure show a potential application in detecting low-frequency AC magnetic field. The details of measurements, results and analysis are presented below.

2. Experiment details

Figure 1 shows the configuration in our experiment, which consists of a Terfenol-D layer (Gansu Tianxing Rare Earth Functional Materials Co., Ltd) and three PZT layers (Shouguang Field Food Co., Ltd). The dimensions of Terfenol-D are 12 mm × 5 mm × 0.5 mm. There are two sizes of PZT layers: 20 mm × 5 mm × 0.3 mm and 30 mm × 5 mm × 0.3 mm, the two piezoelectric layers outside have the same size, and they are longer than the inside one. The Terfenol-D layer is magnetized along the longitudinal direction and the three PZT layers are polarized in the thickness direction. The trestle is of ABS resin, which is nonmagnetic

*Project supported by the National Natural Science Foundation of China (Grant Nos. 11702120, 11372120, 11421062, and 11572143) and the Fundamental Research Funds for the Central Universities, China (Grant No. lzujbky-2016-106).

†Corresponding author. E-mail: zhangjuanjuan@lzu.edu.cn

© 2018 Chinese Physical Society and IOP Publishing Ltd

and nonelectric. It is hinged with a woody pin in the middle of the trestles, therefore, it will not change the magnetic field distribution of the structure. Then we cut eight grooves in the trestle, the ends of Terfenol-D and PZT layers are embedded in the grooves of the trestle, finally pour the 502 adhesive into the grooves. Here the Terfenol-D and PZT layers are parallel to each other. The sample is placed at room temperature for 24 h for an effective bonding between the trestle and components

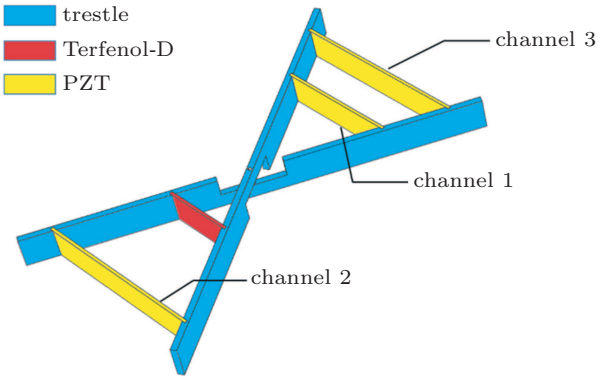


Fig. 1. (color online) Schematic diagram of the sample and the arrangement of three channels.

In order to measure the induced voltage of the ME structure, the applied magnetic field is parallel to the length of Terfenol-D layer. When the ME structure is subjected to an external magnetic field, first, the length of magnetostrictive layer increases, and then the angle of the trestle changes. Because the stiffness of the trestle is large enough to bear the bending moment, thus the PZT layers will be stretched along the length direction. Finally, the induced voltage can be acquired due to the piezoelectric effect of piezoelectric material. That is, a Terfenol-D layer can drive the three PZT layers indirectly by the end bonding of the trestle.

The experiment is carried out at room temperature. The experimental setup for measuring ME voltage signal is displayed in Fig. 2(a), and the detail of circuit connection is plotted in Fig. 2(b). During the experiment, the ME structure is placed in the center of a pair of Helmholtz coils, which is used to generate a small AC magnetic field (H_{ac}). For enhancing the ME coefficient, a direct current (DC) magnetic field (H_{dc}) is needed, which is provided by an electromagnet (WD-130) and parallel to the length direction of Terfenol-D layer. The magnetic field is measured by a Gauss-meter (Lakeshore 475 DSP). A signal generator (Atten ATF208) and an AC power amplifier (HFVA-62) are used to provide a controllable input current for the Helmholtz coils. In this experiment, the AC current is controlled at 0.328 A to keep the effective value of AC magnetic field at 1 Oe. Then the output voltage of ME structure is measured with an oscilloscope (Agilent DSO9064A). Three individual channels are chosen to measure the ME output voltages of three piezoelectric layers as shown in Fig. 1(a).

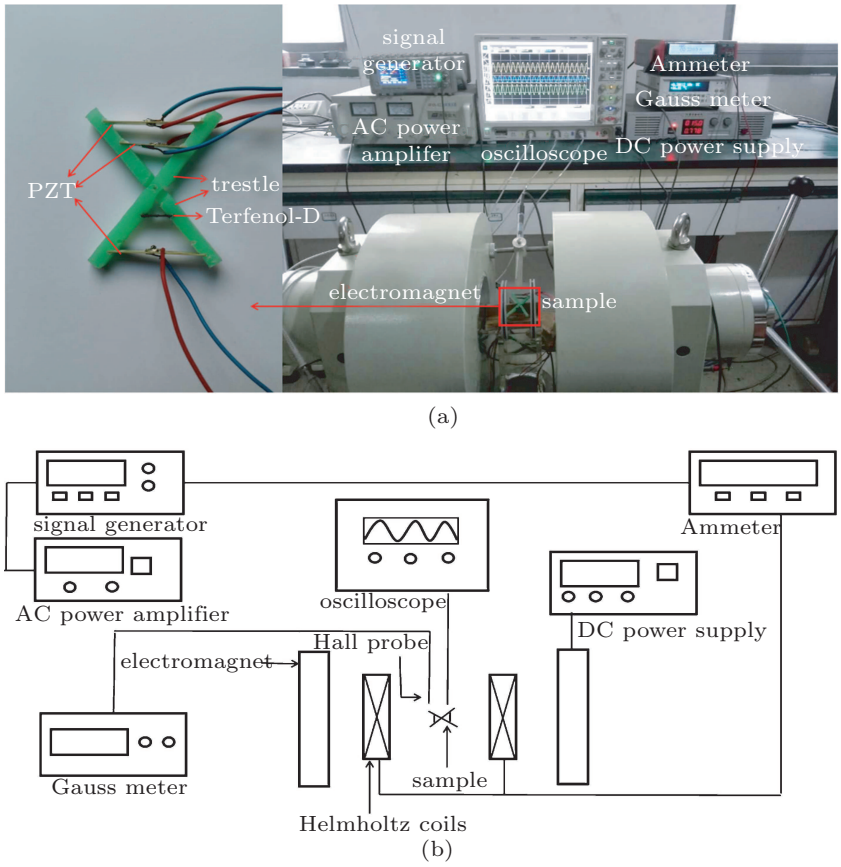


Fig. 2. (color online) Sample and schematic diagram of measurement system; (b) detail of circuit connection.

3. Results and discussion

At first, we measure the real-time voltage signals of three piezoelectric layers from three channels separately as shown in Fig. 3. It is found that the curves are all sinusoidal or cosinoidal, and the amplitudes of the output voltages remain relative stable. Meanwhile, the phase difference can be observed among the three channels. In Fig. 3(a), the amplitude of the output voltage in channel 1 is larger than those of other two channels while the applied magnetic field and frequency are the same. From Fig. 3(b), the phase difference becomes more obvious than that in Fig. 3(a). For example, when a maximum value of the output voltage appears in channel 2, the output voltages are observed in channels 1 and 3 to be minimum values. The amplitudes and phases of the output voltages in three channels are different under different conditions, which can be attributed to the fact that the resonant frequencies of three piezoelectric layers change with external condition, because the resonant frequency is related to the material parameter and the wave source.[14]

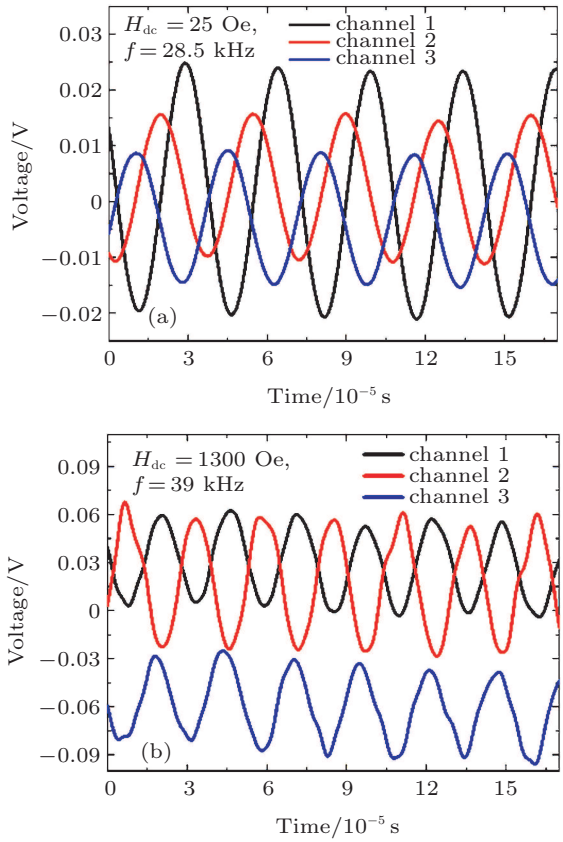


Fig. 3. (color online) Transient output voltages from three piezoelectric layers at (a) $H_{dc} = 250$ Oe and $f = 28.5$ kHz and (b) $H_{dc} = 1300$ Oe and $f = 39$ kHz.

The variations of the ME coefficients with magnetic field frequency are shown in Fig. 4. The ME coefficient is calculated by using the expression $\alpha_E^i = V_{p-p}^i/(H_{ac}t_p^i)$ ($i = 1, 2, 3$, are the channel numbers), where V_{p-p}^i is the peak–peak value of the ME output voltage, H_{ac} is the effective value of AC magnetic field and t_p^i is the thickness of each piezoelectric layer.[24] The values of DC magnetic field are set to be 128 Oe, 302 Oe, and 1000 Oe, the frequency range is in a range of 1 kHz–200 kHz. It can be seen that the multi-frequency phenomenon in each of the three channels can be observed, and the tendency in a channel is almost the same under different applied magnetic fields. While the ME coefficients in a channel varies with the applied magnetic field. Besides, the frequency shift can be observed when the proposed structure is in resonance. For example, when the DC magnetic field is 302 Oe, the resonant of the proposed structure is 28.5 kHz in channel 1, it shifts to 27.5 kHz when $H_{dc} = 128$ Oe and 27 kHz when $H_{dc} = 1000$ Oe. Moreover, the bandwidth of the ME structure is widened under different DC magnetic fields. For instance, the ME coefficient in channel 2 keeps a relatively high value in a frequency range of 12 kHz–61 kHz. It may be useful in designing the broadband ME energy harvester.

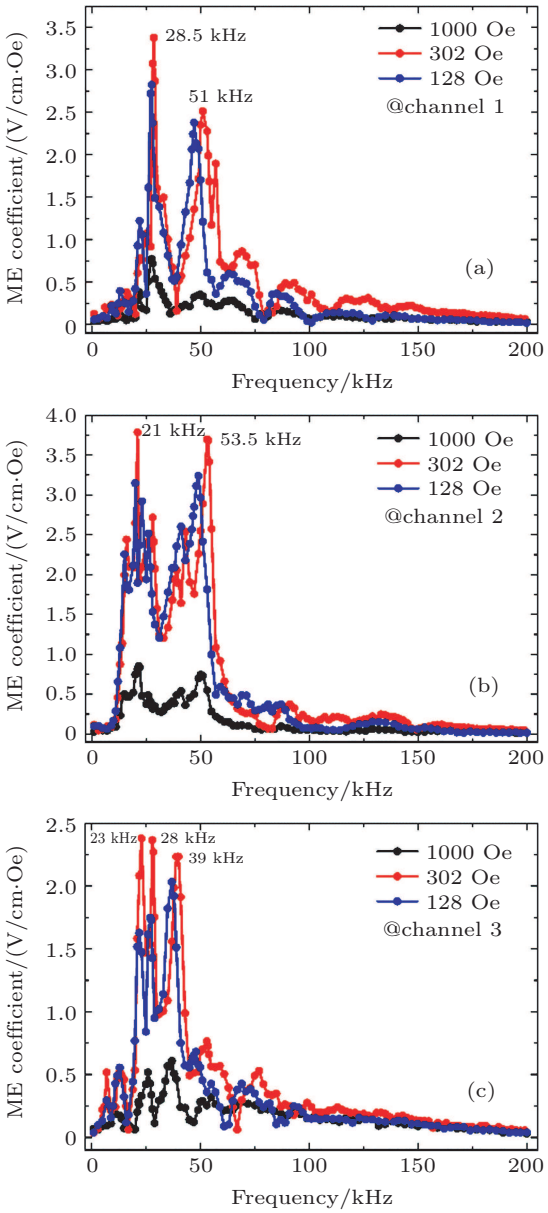


Fig. 4. (color online) The frequency-dependent α_E at different magnetic fields in (a) channel 1, (b) channel 2, and (c) channel 3.

Table 1. ME properties of the ME structure extracted from Fig. 4.

ME properties	Channel 1	Channel 2	Channel 3
Maximum value of α_E	3.38 V/cm·Oe	3.78 V/cm·Oe	2.38 V/cm·Oe
Number of peaks ($H_{dc} = 302$ Oe $\alpha_E \geq 0.5$ V/cm·Oe)	3	6	3
Maximum frequency range ($H_{dc} = 302$ Oe $\alpha_E \geq 0.5$ V/cm·Oe)	21 kHz∼38 kHz 40 kHz∼75 kHz	13 kHz∼61 kHz	20 kHz∼61 kHz

Figure 5 shows the variations of α_E with frequency when the bias magnetic field is 302 Oe, the frequency range is in a range of 1 kHz–200 kHz. It is clear that all channels present several sharp peaks with the increase of frequency. The multi-peaks can be attributed to the multiple vibration modes of the structure. Since the adjacent resonant frequencies overlap each other, which causes the ME coefficient to maintain a relatively high value within a broad band. By picking up the largest value in three channels over the frequency of 1 kHz–200 kHz, the curve of α_E versus f is redrawn in Fig. 5(b). It can be seen that the ME coefficient is greater than 0.5 V/cm·Oe over the frequency of 12 kHz–77 kHz the bandwidth reaches 65 kHz. That is to say we can obtain a larger ME coefficient by choosing a right channel. The results indicate that the ME structure may have potential applications in multifunctional device for multi-frequency operation.

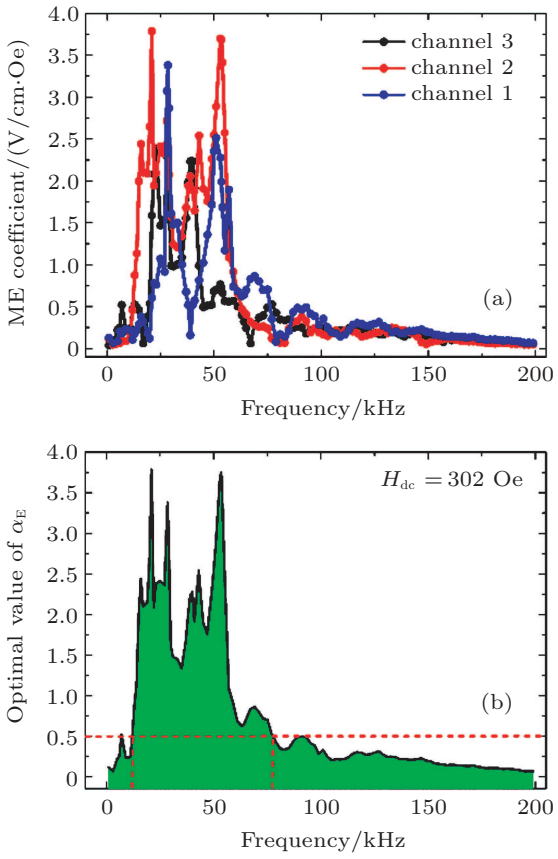


Fig. 5. (color online) (a) Variations of ME coefficient of the structure and (b) the optimal value of α_E with frequency at $H_{dc} = 302$ Oe.

Figure 6 shows plots of ME coefficient versus cyclic magnetic field under a resonant frequency ($f = 28.5$ kHz). It can be seen that the curves are nonlinear and the hysteresis characteristics appear. Those curves are similar in shape, because the piezoelectric layers are driven by the same Terfenol-D layer. Under the action of a cyclic magnetic field, the hysteresis characteristic of Terfenol-D layer leads to a nonzero magnetization when the applied magnetic field decreases from saturation magnetic field to zero, which means that a relatively large coercive field exists in the Terfenol-D layer, then the hysteresis hoops in three channels appear.[25] However, the magnitudes of α_E in three channels are different due to the different geometry sizes of piezoelectric layers and the distances from the Terfenol-D layer.

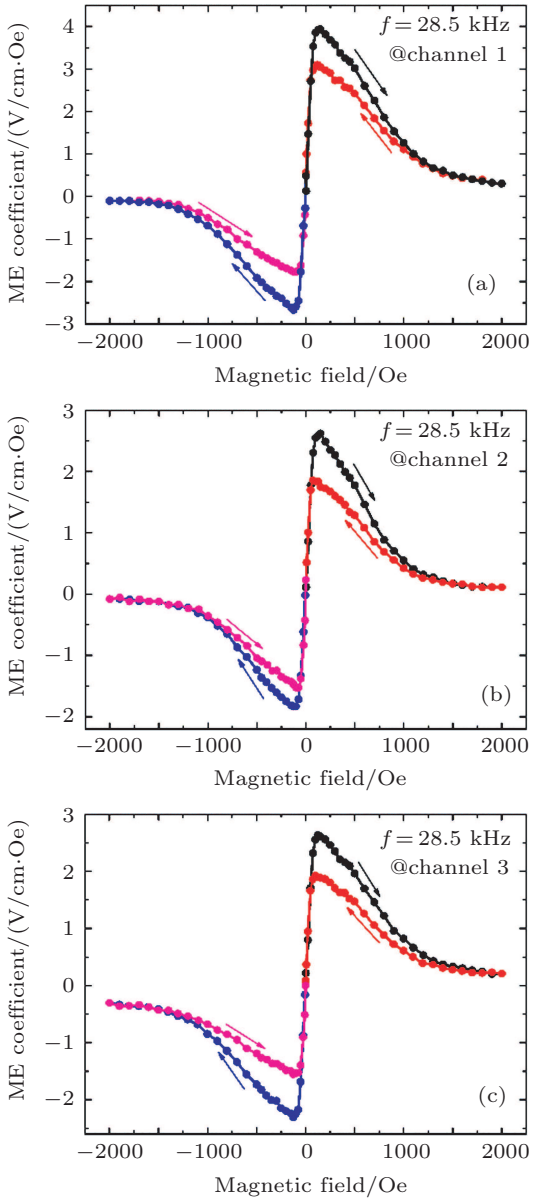


Fig. 6. (color online) Magnetic field-dependent ME coefficients of channels 1 (a), 2 (b), and 3 (c) under $f = 28.5$ kHz.

In order to study the influence of the frequency on ME coefficient, we measure the ME coefficients at three different frequencies and in a magnetic field range from 0 to 2000 Oe. Figure 7 shows α_E versus H_{dc} curves at three resonant frequencies. The curves have similar tendencies. Each of the ME coefficients first increases and then reaches a maximum value, with the further increase of DC magnetic field, it decreases rapidly to a minimum value. The optimal magnetic field is about 150 Oe. The values of α_E in three channels are different at an identical frequency, and α_E in a channel varies with frequency changing The maximum values of α_E appear in different channels at different resonant frequencies, and the results are listed in Table 2. For example, α_E reaches a peak value of 3.95 V/cm·Oe in channel 2 when $f = 21$ kHz, and the sequence of α_E^{max} is ${}^2\alpha_E^{max} > {}^1\alpha_E^{max} > {}^3\alpha_E^{max}$. While the maximum value of α_E is 3.93 V/cm·Oe and occurs in channel 1 when $f = 28.5$ kHz, and the sequence of α_E^{max} is ${}^1\alpha_E^{max} > {}^3\alpha_E^{max} > {}^2\alpha_E^{max}$.

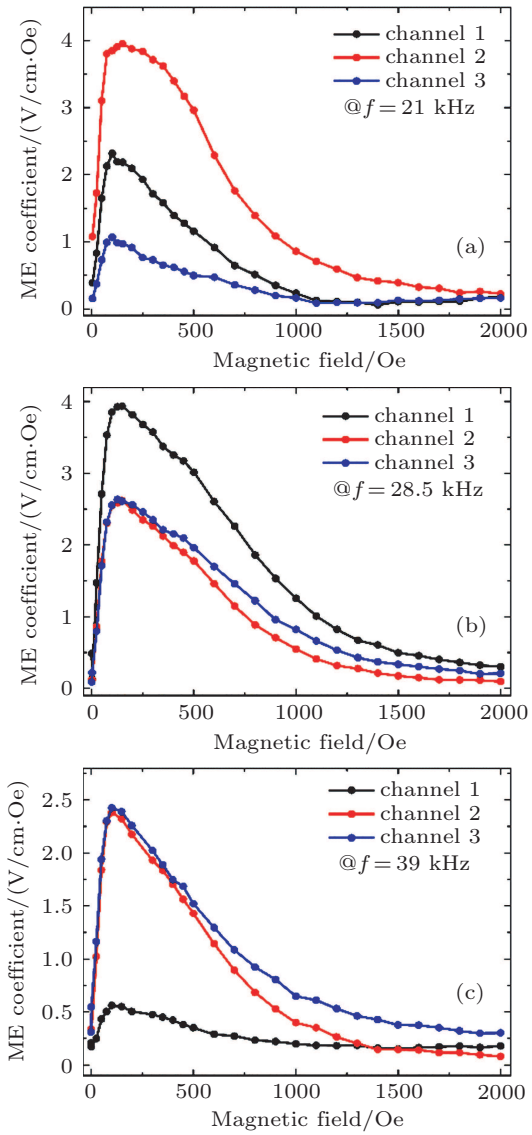


Fig. 7. (color online) Plots of ME coefficient versus magnetic field at frequencies of (a) 21 kHz, (b) 28.5 kHz, and (c) 39 kHz.

Table 2. Values of α_E^{max} under different frequencies in various channels.

	${}^1\alpha_E^{max}$	${}^2\alpha_E^{max}$	${}^3\alpha_E^{max}$	Sequence
21 kHz	1.26	3.95	0.72	${}^2\alpha_E^{max} > {}^1\alpha_E^{max} > {}^3\alpha_E^{max}$
28.5 kHz	3.93	2.62	2.63	${}^1\alpha_E^{max} > {}^3\alpha_E^{max} > {}^2\alpha_E^{max}$
39 kHz	0.72	2.46	2.42	${}^2\alpha_E^{max} > {}^3\alpha_E^{max} > {}^1\alpha_E^{max}$

To explain the phenomena mentioned above, a finite element modeling analysis based on a commercial software COMSOL Multiphysics is performed to estimate the resonant frequency of the structure. The simulation is performed by utilizing the piezoelectric devices (PZD) module, and the detail of calculation process is presented in the Appendix. The modeling results are presented in Fig. 8. Firstly, we calculate the mode shape of the proposed structure. Actually, the displacement in the proposed structure is small, for a better display, the displacement is magnified by a magnification factor ($\sim 10^8$ times), the nephograms of mode shape in Figs. 8(a)–8(c) correspond to the three resonant frequencies listed in Table 2, respectively. It can be seen clearly from Table 3 that the displacement u^{max} sequence is consistent well with the α_E^{max} sequence in Table 2. For instance, when the resonant frequency is 21 kHz, the sequence of α_E^{max} is ${}^2\alpha_E^{max} > {}^1\alpha_E^{max} > {}^3\alpha_E^{max}$

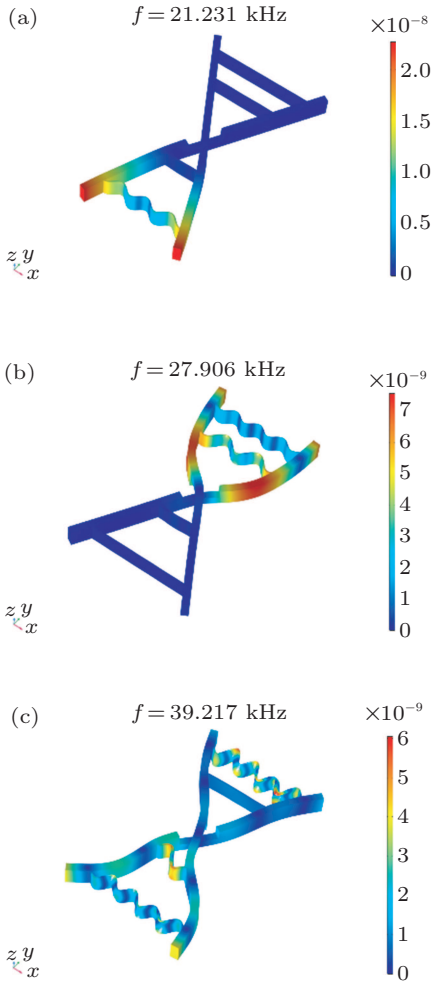


Fig. 8. (color online) Mode shape analyses as a function of frequency in three piezoelectric layers.

while the sequence of $u^{\max}$ is ${}^{2}u^{\max} > {}^{1}u^{\max} > {}^{3}u^{\max}$. It is indicated that the positions of local resonance are different at different resonant frequencies.

Table 3. Values of $u^{\max}$ at different frequencies in various PZT plates.

	${}^{1}u^{\max}$	${}^{2}u^{\max}$	${}^{3}u^{\max}$	Sequence
21.231 kHz	0.0302	2.5863	0.0084	${}^{2}u^{\max} > {}^{1}u^{\max} > {}^{3}u^{\max}$
27.906 kHz	2.7794	0.0450	1.2623	${}^{1}u^{\max} > {}^{3}u^{\max} > {}^{2}u^{\max}$
39.217 kHz	0.3317	3.4260	2.0823	${}^{2}u^{\max} > {}^{3}u^{\max} > {}^{1}u^{\max}$

Figure 9 shows the plot of ME voltage versus frequency for the ME structure. Here a couple of stresses of 800 N/m^2 is exerted on the two ends of Terfenol-D plate. It can be seen that the resonant frequencies in simulation are generally in good agreement with the measurement results in Fig. 4. For a numerical comparison, we take one of three groups of data for example. The simulation result in Fig. 9(b) shows relatively high resonant peaks at frequencies of 12.5, 21, 30.5, 35, 39, 47, 54.5, 62, 65, 79, and 87.5 kHz. Meanwhile, The ME coefficients in Fig. 4(b) demonstrate resonant peaks at 15, 2, 26, 41, 49, 59, 69, 81, and 87 kHz when the external magnetic field is 128 Oe. There is a little difference between experiment data and simulation results. The discrepancy may be caused by the friction force between two trestles, which is ignored in finite element modeling. It is indicated that electromechanical resonant modes are responsible for the multiple resonant peaks.

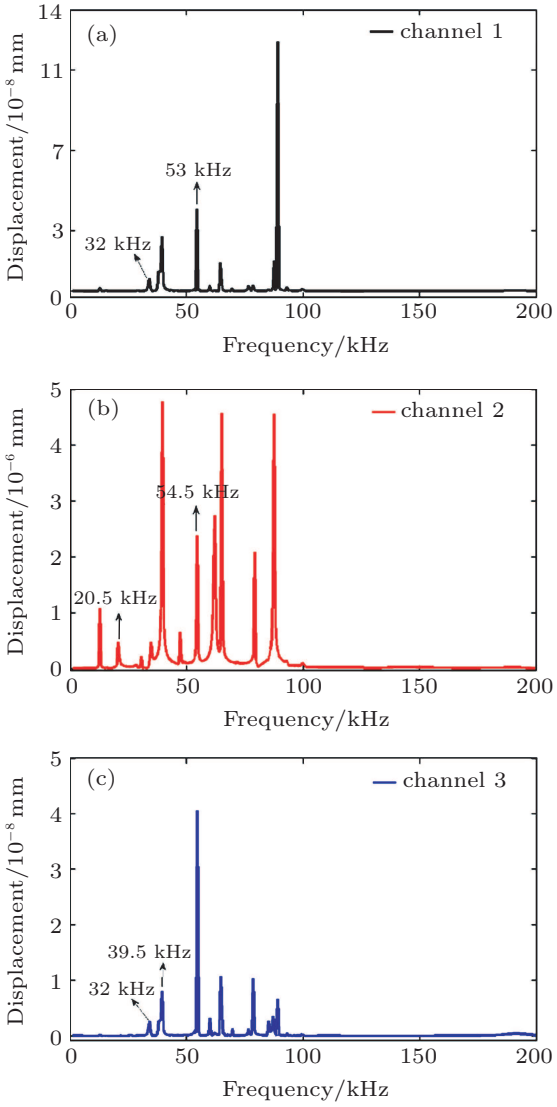


Fig. 9. (color online) Plots of output voltage versus frequency in three piezoelectric layers.

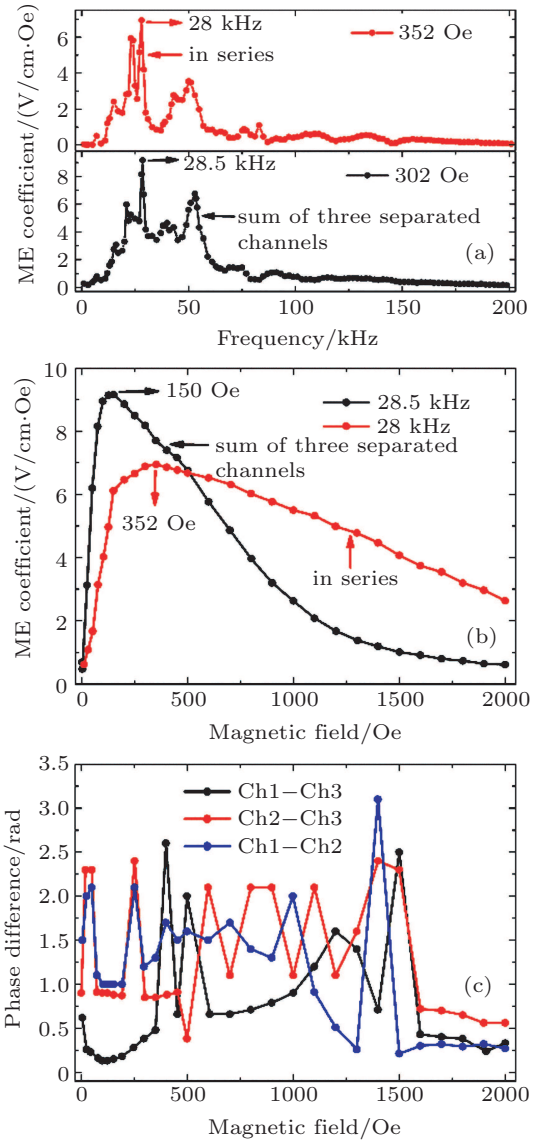


Fig. 10. (color online) Comparison between (a) the frequency-dependent and (b) the magnetic field-dependent ME coefficients under different electric connections; (c) the variations of phase difference with magnetic field.

Finally, the ME response of the structure by connecting three piezoelectric plates in series is studied. Here we compare the result in series with the superposition of three separate channels as shown in Figs. 10(a) and 10(b). The bandwidth of two curves in Fig. 10(a) is almost the same. However, the resonant frequency has a slightly difference when the electric connection changes (the resonant frequency is 28 kHz for channels in series, and 28.5 kHz for the superimposed channel). Meanwhile, the optimal magnetic field changes in different electric connections as shown in Fig. 10(b). When three

channels are measured separately at $f = 28.5$ kHz, the optimal magnetic field is 150 Oe, but it shifts to 352 Oe when they are connected in series. The maximum value of the ME coefficient increases to 6.94 V/cm·Oe at $f = 28$ kHz when three channels are connected in series, which is larger than that of any single channel in Fig. 7. Nevertheless, it is still lower than the sum of maximum values of three separate channels, in which the maximum value of the ME coefficient is 9.16 V/cm·Oe. We speculate that the phase difference is one of the main factors causing the the ME coefficient to diminish, just as the case shown in Fig. 3(b), the maximum value appears in channel 2 while the minimum value occur in channels 1 and 3. In addition, the variations of phase difference with magnetic field are plotted in Fig. 10(c). There is no rule can be obtained from those curves, but the phase difference exists among channels all the time, which verifies our assumption.

4. Conclusions

In this work, a novel ME structure is developed, which is made up of one Terfenol-D layer and three PZT layers, and the three PZT layers can be driven by one Terfenol-D layer simultaneously. The multiple resonant frequencies and broad bandwidth characteristics of the proposed structure are investigated by experimental method and finite element modeling. The experimental results show that the proposed structure can maintain good performance in a wide bandwidth due to the adjacent resonant frequencies overlap each other. The results provide an alternative way of designing multi-frequency energy harvesters. Moreover, the sequences of $\alpha_{\mathrm{E}}^{\max}$ values in three channels are different at an identical resonant frequency, and the simulation results illustrate that the position of local resonance changes with resonant frequency. Besides, the ME coefficient hysteresis hoop can be obtained from three channels due to the hysteresis characteristic of the Terfenol-D layer. In addition, the ME coefficient in series mode is not the simple sum of three channels, because the phase differences exist among three channels.

Appendix A

In order to validate our experimental results, a finite element model is built in COMSOL Multiphysics. The simulation is conducted by utilizing the PZD module, an eigen frequency solver and a frequency domain solver. The geometric dimension is based on experimental sample.

The trestle material properties are chosen as $E = 200$ GPa, $v = 0.35$, and $\rho = 3200\ \mathrm{kg/m^3}$. For the Terfenol-D layer, material parameters are $E^m = 80$ GPa, $v^m = 0.3$, and $\rho^m = 9400\ \mathrm{kg/m^3}$. The piezoelectric layers are considered to be of anisotropic material, and its density is $\rho^{\mathrm{p}} = 7500\ \mathrm{kg/m^3}$. The compliance coefficients s_{ij}^{p}, piezoelectric charge constant d_{ij}^{p} and relative permittivity $\varepsilon_{ij}^{\mathrm{p}}$ in matrix form are listed as follows:

$$s_{ij}^{\mathrm{p}} = \begin{bmatrix} 16.5 & -4.78 & -8.45 & 0 & 0 & 0 \\ -4.78 & 16.5 & -8.45 & 0 & 0 & 0 \\ -8.45 & -8.45 & 20.7 & 0 & 0 & 0 \\ 0 & 0 & 0 & 43.5 & 0 & 0 \\ 0 & 0 & 0 & 0 & 43.5 & 0 \\ 0 & 0 & 0 & 0 & 0 & 42.6 \end{bmatrix} \times 10^{-12}\ \mathrm{m^2/N}, \tag{A1}$$

$$d_{ij}^{\mathrm{p}} = \begin{bmatrix} 0 & 0 & 0 & 0 & 741 & 0 \\ 0 & 0 & 0 & 741 & 0 & 0 \\ -274 & -274 & 593 & 0 & 0 & 0 \end{bmatrix} \times 10^{-12}\ \mathrm{C/N}, \tag{A2}$$

$$\frac{\varepsilon_{ij}^{\mathrm{p}}}{\varepsilon_0} = \begin{bmatrix} 3130 & 0 & 0 \\ 0 & 3130 & 0 \\ 0 & 0 & 3400 \end{bmatrix}, \tag{A3}$$

$$\varepsilon_0 = 8.854 \times 10^{-12}\ \mathrm{F/m}.$$

References

[1] Scott J F 2012 *J. Mater. Chem.* **22** 4567
[2] Liu G, Ci P and Dong S X 2014 *Appl. Phys. Lett.* **104** 032908
[3] Ryu J, Kang J E, Zhou Y, Choi S Y, Yoon W H, Park D S, Choi J J, Hahn B D, Ahn C W and Kim J W 2015 *Energ. Environ. Sci.* **8** 2402
[4] Bi K, Wang Y G, Wu W, Gu Q L and Cui H N 2011 *J. Alloys Compd.* **509** 5163
[5] Pan D A, Bai Y, Volinsky A A, Chu W Y and Qiao L J 2008 *Appl. Phys. Lett.* **92** 052904
[6] Lv X, Or S W, Liu W, Liu X and Zhang Z 2009 *J. Alloys Compd.* **476** 271
[7] Jiang Q H, Shen Z J, Zhou J P, Shi Z and Nan C W 2011 *J. Eur. Ceram. Soc.* **27** 279
[8] Srinivasan G, Devreugd C P, Flattery C S, Laletsin V M and Paddubnaya N 2004 *Appl. Phys. Lett.* **85** 2550
[9] Fang F, Zhou Y Y, Xu Y T, Jing W Q and Yang W 2013 *Smart. Mater. Struct.* **22** 75009
[10] Qiu J, Wen Y M, Li P and Chen H 2014 *Appl. Phys. Lett.* **104** 112401
[11] Jia Y M 2015 *Appl. Sci.* **5** 587
[12] Zhai J, Dong S X, Xing Z, Li J and Viehland D 2006 *Appl. Phys. Lett.* **89** 083507
[13] Zeng L, Zhou M, Bi K and Lei M 2016 *J. Appl. Phys.* **119** 034102
[14] Yang C, Li P, Wen Y M, Lu C J, Yang A, Wang D, Zhang J and Zhang F 2014 *IEEE T. Magn.* **50** 1
[15] Fang F, Jing W, Zhou Y and Yang W 2014 *J. Eur. Ceram. Soc.* **97** 2511
[16] Li L, Lin Y Q and Chen X M 2007 *J. Appl. Phys.* **102** 064103
[17] Yu H, Zeng M, Wang Y and Wan J G 2005 *Appl. Phys. Lett.* **86** 032508
[18] Xu L R, Pan D A, Zuo Z J, Wang J, Volinsky A A and Qiao L J 2015 *Appl. Phys. Lett.* **106** 032904
[19] Huang D, Lu C and Bing H 2015 *AIP Adv.* **5** 031101
[20] Park C S and Priya S 2012 *Adv. Cond. Mater. Phys.* **2012** 323165
[21] Zhang J J, Kang Y, Yu Y and Gao Y W 2016 *Phys. Lett. A* **381** 1
[22] Cheng J H, Wang Y G and Xie D 2014 *Appl. Phys. Lett.* **104** 252411
[23] Patil D R, Kambale R C, Chai Y, Yoon W H, Jeong D Y, Park D S, Kim J W, Choi J J, Ahn C W and Hahn B D 2013 *Appl. Phys. Lett.* **103** 052907
[24] Fang F, Shan S C and Yang W 2010 *J. Appl. Phys.* **108** 104505
[25] Huber J E, Fleck N A, Landis C M and Mcmeeking R M 1999 *J. Mech. Phys. Solids* **47** 1663